

## Electronic supplementary information

### <sup>14</sup>N Solid-State NMR: A sensitive probe of the local order in zeolites

Eddy Dib,<sup>a</sup> Tzonka Mineva,<sup>a</sup> Philippe Gaveau<sup>a</sup> and Bruno Alonso\*<sup>a</sup>

<sup>a</sup>ICGM-MACS, UMR 5253 CNRS-ENSCM-UM2-UM1, Institut Charles Gerhardt de Montpellier, 8 rue de l'Ecole normale,  
34296 Montpellier cedex 5, France.

#### 1. Additional experimental details

##### 1.1 Syntheses

The syntheses and the post-synthetic treatments were carried out following known procedures.<sup>1,2,3</sup>

**F-MFI**: the initial gel composition was 1 SiO<sub>2</sub> : 0.08 TPABr : 0.04 NH<sub>4</sub>F : 20 H<sub>2</sub>O, the resulting mixture was heated in a PTFE-lined autoclave at 473 K for 15 days. **OH-MFI**: the initial gel composition was 1 SiO<sub>2</sub> : 0.43 TPAOH : 28 H<sub>2</sub>O, the resulting mixture was heated in a PTFE-lined autoclave at 448 K for 2 days. The as-synthesized materials were recovered by filtration and dried over night at 353 K. **HT-F-MFI**: the post-treatment of F-MFI was done in an PTFE-lined autoclave at 448 K for 4 days using a 0.07 wt% NH<sub>4</sub>OH aq. solution. Elemental analyses, NMR and thermogravimetric data are consistent with the compositions: F-MFI (1 SiO<sub>2</sub> : 0.04 TPA<sup>+</sup> : 0.04 F<sup>-</sup>), OH-MFI (1 SiO<sub>2</sub> : 0.04 TPA<sup>+</sup> : 0.04 OH<sup>-</sup>), HT-F-MFI (1 SiO<sub>2</sub> : 0.04 TPA<sup>+</sup> : 0.04 F<sup>-</sup>).

##### 1.2 SEM and XRD characterisation

The Scanning Electron Microscopy (SEM) was undertaken using a HITACHI 4800 S microscope and metallised samples. X-Ray diffraction (XRD) powder patterns were collected on a Bruker AXS D8 diffractometer using Cu-K<sub>α</sub> radiation.

##### 1.3 NMR methods

###### **<sup>13</sup>C NMR**

<sup>13</sup>C{<sup>1</sup>H} NMR cross-polarization (CP) MAS spectra were recorded on a Varian 600 MHz spectrometer operating at a magnetic field of 14.1 T (<sup>13</sup>C Larmor frequency of 150.98 MHz) using 9.5 mm rotors. Experiments were conducted using: contact times of 5 ms, a linear ramp on the <sup>1</sup>H contact pulse (10 % slope), <sup>1</sup>H decoupling during acquisition (<sup>1</sup>H nutation frequency of 50 kHz), and recycle delay of 5 s. <sup>13</sup>C NMR chemical shifts were referenced towards external neat TMS.

<sup>13</sup>C Chemical Shift Anisotropy (CSA) parameters were obtained by modelling the spectra recorded at low MAS frequency (1.5 and 2.0 kHz). The CSA interaction tensor is defined by the isotropic chemical shift  $\delta_{iso}$ , the anisotropy  $\Delta_{CSA}$  and the asymmetry  $\eta_{CSA}$  parameters, defined here by:

<sup>1</sup> J.L. Guth, H. Kessler, J. M. Higel, J. M. Lamblin, J. Patarin, A. Seive, J. M. Chezeau and R. Wey, *J. Am. Chem. Soc.*, 1988, **196**, 238.

<sup>2</sup> H. Koller, R. F. Lobo, S. L. Burkett and M. E. Davis, *J. Phys. Chem. A.*, 1995, **99**, 12588-12596.

<sup>3</sup> X. L. Liu, U. Ravon and A. Tuel, *Angew. Chem., Int. Ed.*, 2011, **50**, 5900-5903.

$$\delta_{iso} = (\delta_{11} + \delta_{22} + \delta_{33}) / 3 ; \Delta_{CSA} = (\delta_{33} - \delta_{iso}) ; \eta_{CSA} = (\delta_{22} - \delta_{11}) / (\delta_{33} - \delta_{iso})$$

where  $|\delta_{33} - \delta_{iso}| > |\delta_{11} - \delta_{iso}| > |\delta_{22} - \delta_{iso}|$ .

### **<sup>29</sup>Si NMR**

<sup>29</sup>Si{<sup>1</sup>H} NMR CP-MAS spectra were recorded on a Varian 400 MHz spectrometer operating at a magnetic field of 9.4 T (<sup>29</sup>Si Larmor frequency of 79.55 MHz) using 7.5 mm rotors. Experiments were conducted using: contact times of 15 ms, a linear ramp on the <sup>1</sup>H contact pulse (10 % slope), <sup>1</sup>H decoupling during acquisition (<sup>1</sup>H nutation frequency of 50 kHz), and recycle delay of 2 s. <sup>29</sup>Si NMR chemical shifts were referenced towards external neat TMS.

### **<sup>14</sup>N NMR**

<sup>14</sup>N NMR MAS single pulse spectra were recorded at the Larmor frequency of 43.33 MHz on widebore 600 Varian Spectrometer ( $B_0 = 14.1$  T) using 9.5 mm rotors spun at  $\nu_{MAS} = 2, 3$  and 4 kHz. RF field strengths  $\nu_{RF}$  were set to ca. 42 kHz, flip angles to  $\pi/4$  (6  $\mu$ s, bandwidth ~85 kHz) and recycling delays to 0.5 s. Smaller flip angles were also tested (down to 2  $\mu$ s, bandwidth ~250 kHz). These conditions insure a wide irradiation, and proper longitudinal relaxation. The FID was left shifted so as to consider only the acquired points after the first rotational echo maximum. <sup>1</sup>H decoupling ( $\nu_{RF} \sim 25$  kHz) was used during <sup>14</sup>N acquisition. <sup>14</sup>N NMR chemical shifts were referenced towards solid NH<sub>4</sub>Cl spun at 3 kHz. For the magic angle setting, we use the <sup>14</sup>N NMR signal of tetramethylammonium bromide as standard. The MAS frequencies were stable within 1-2 Hz.

The <sup>14</sup>N nuclear quadrupolar coupling interaction tensor is described by the quadrupolar coupling constant  $C_Q$  and the asymmetry parameter  $\eta_Q$  defined by the principal values  $V_{ii}$  of the Electric Field Gradient (EFG) tensor following:

$$C_Q = eQV_{33} / h ; \eta_Q = (V_{22} - V_{11}) / V_{33}$$

where  $V_{33} = eq ; V_{33} + V_{22} + V_{11} = 0$  and  $|V_{33}| > |V_{11}| > |V_{22}|$ .

### **NMR Spectrum Modelling**

NMR spectra were modelled done using the freely available *DmFit* software.<sup>4</sup> The <sup>13</sup>C and <sup>29</sup>Si NMR spectra were modelled using Lorentzian or Gaussian functions (that can take into account the spinning sidebands in the “CSA” function in the *DmFit* software). <sup>14</sup>N NMR MAS spectra were modelled considering single sets of quadrupolar parameters ( $C_Q, \eta_Q$ ), or Czjcek distributions<sup>5</sup> (respectively “QUAD1st” or “Q1-Cz” functions in the *DmFit* software).

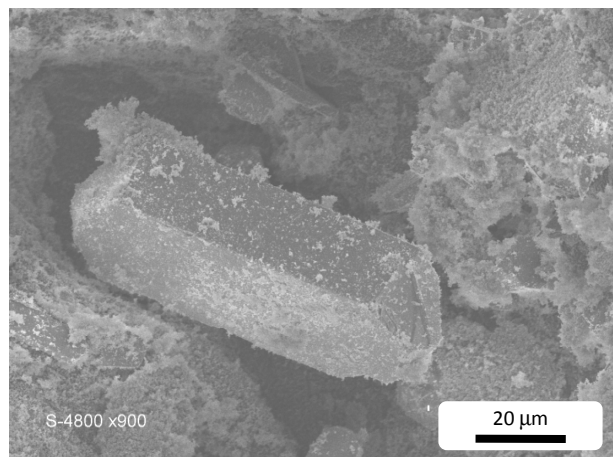
<sup>4</sup> D. Massiot, F. Fayon, M. Capron, I. King, S. L. Calvé, B. Alonso, J.-O. Durand, B. Bujoli, Z. Gan and G. Hoatson, *Magn. Reson. Chem.*, 2002, **40**, 70-76.

<sup>5</sup> D.R. Neuville, L. Cormier and D. Massiot, *Geochim. Cosmochim. Acta*, 2004, **68**, 5071-5079; B. Alonso, D. Massiot, P. Florian, H. H. Paradies, P. Gaveau and T. Mineva, *J. Phys. Chem. B*, 2009, **113**, 11906-11920.

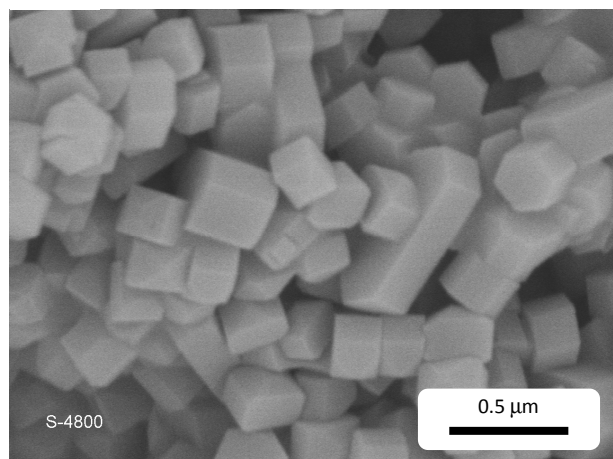
## 2. Scanning Electron Microscopy

**Fig. S1** SEM micrographs of as-synthesised silicalite-1 samples: (a) F-MFI, (b) OH-MFI and (c) HT-F-MFI.

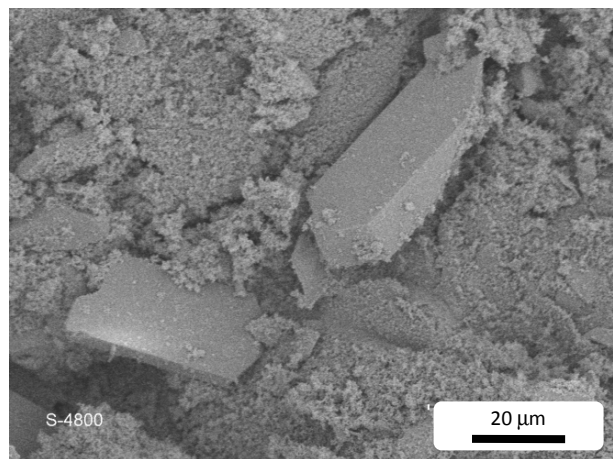
(a)



(b)



(c)



### 3. X-Rays Diffraction patterns

**Fig. S2** XRD patterns of as-synthesised silicalite-1 samples: (a) OH-MFI; (b) F-MFI; (c) HT-F-MFI after treatment with  $\text{NH}_4\text{OH}$  and (d) a model pattern for as synthesized silicalite-1 from [www.iza.org](http://www.iza.org) (the more intense peaks are indexed).

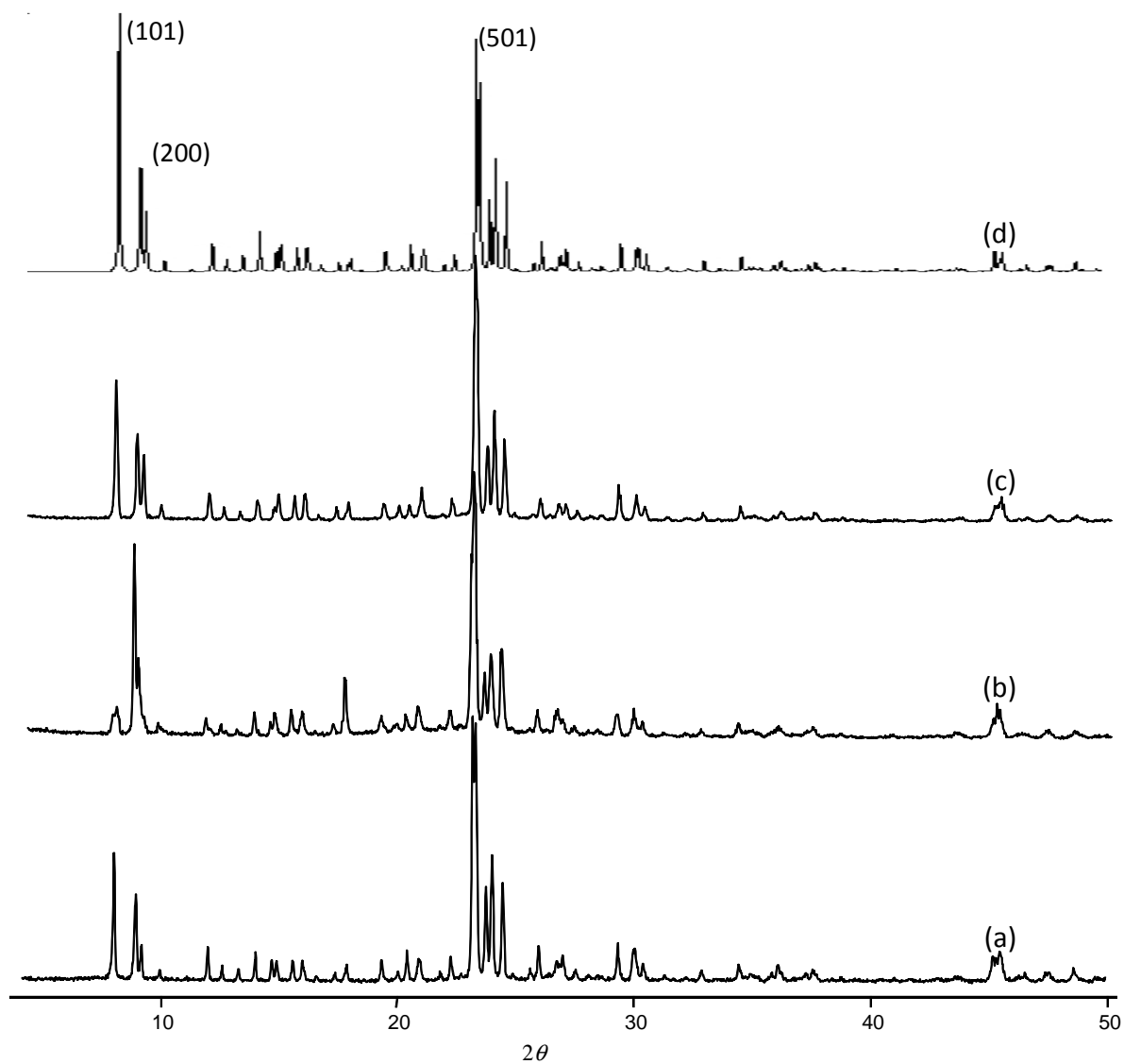
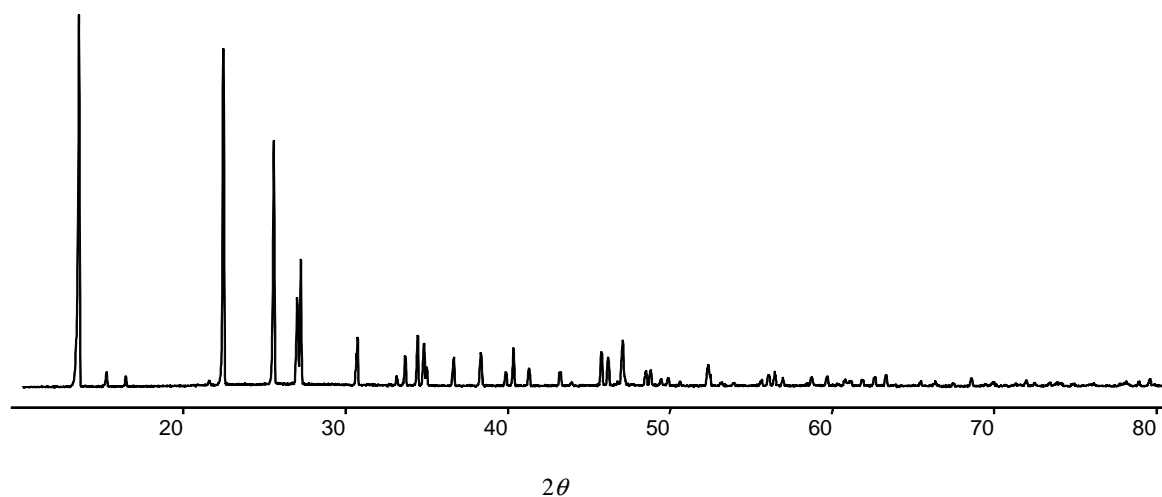


**Fig. S3** XRD pattern of TPABr crystals



#### 4. $^{14}\text{N}$ NMR spectra

**Fig. S4**  $^{14}\text{N}$  spectra of: F-MFI (left); OH-MFI (right) at different MAS frequencies: (a)  $\nu_{\text{MAS}} = 2$  kHz, (b)  $\nu_{\text{MAS}} = 3$  kHz, (c)  $\nu_{\text{MAS}} = 4$  kHz. The experimental spectra ( $8.10^3$  to  $98.10^3$  scans) are shown on the top, the modelled spectra on the middle and the differences between them are shown in the bottom.

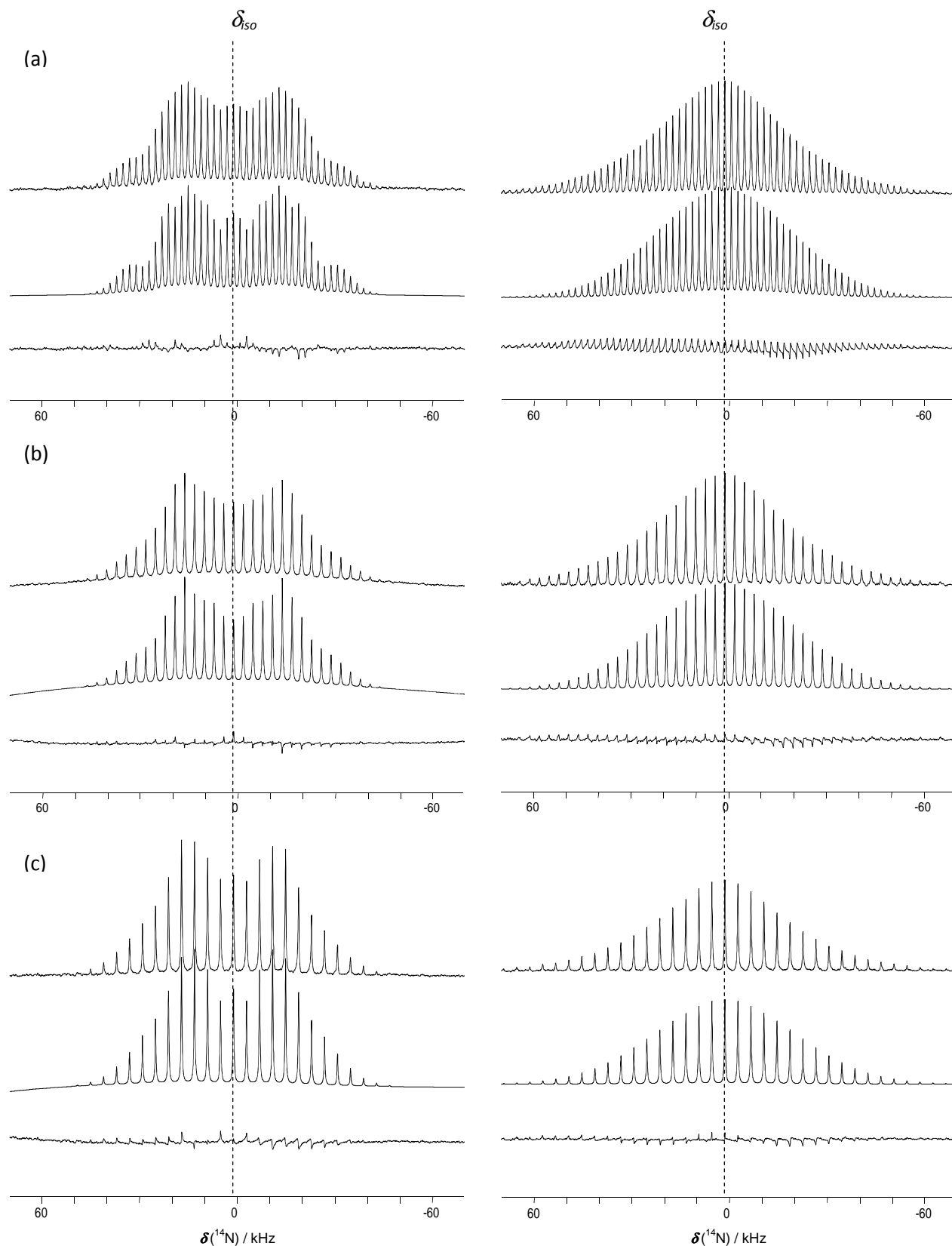


**Fig. S5**  $^{14}\text{N}$  spectra of HT-F-MFI (F-MFI treated with  $\text{NH}_4\text{OH}$ ) at different MAS frequencies: (a)  $\nu_{\text{MAS}} = 2$  kHz, (b)  $\nu_{\text{MAS}} = 3$  kHz, (c)  $\nu_{\text{MAS}} = 4$  kHz. The experimental spectra ( $10^4$  to  $5 \cdot 10^4$  scans) are shown on the top, the modelled spectra on the middle and the differences between experimental and modelled spectra are shown in the bottom. The spectra were modelled using two functions for two different signals. The first signal A corresponds to the initial set of quadrupolar parameters (F-MFI); the second signal B corresponds to a new set of quadrupolar parameters adjusted by the iterative fitting procedure.

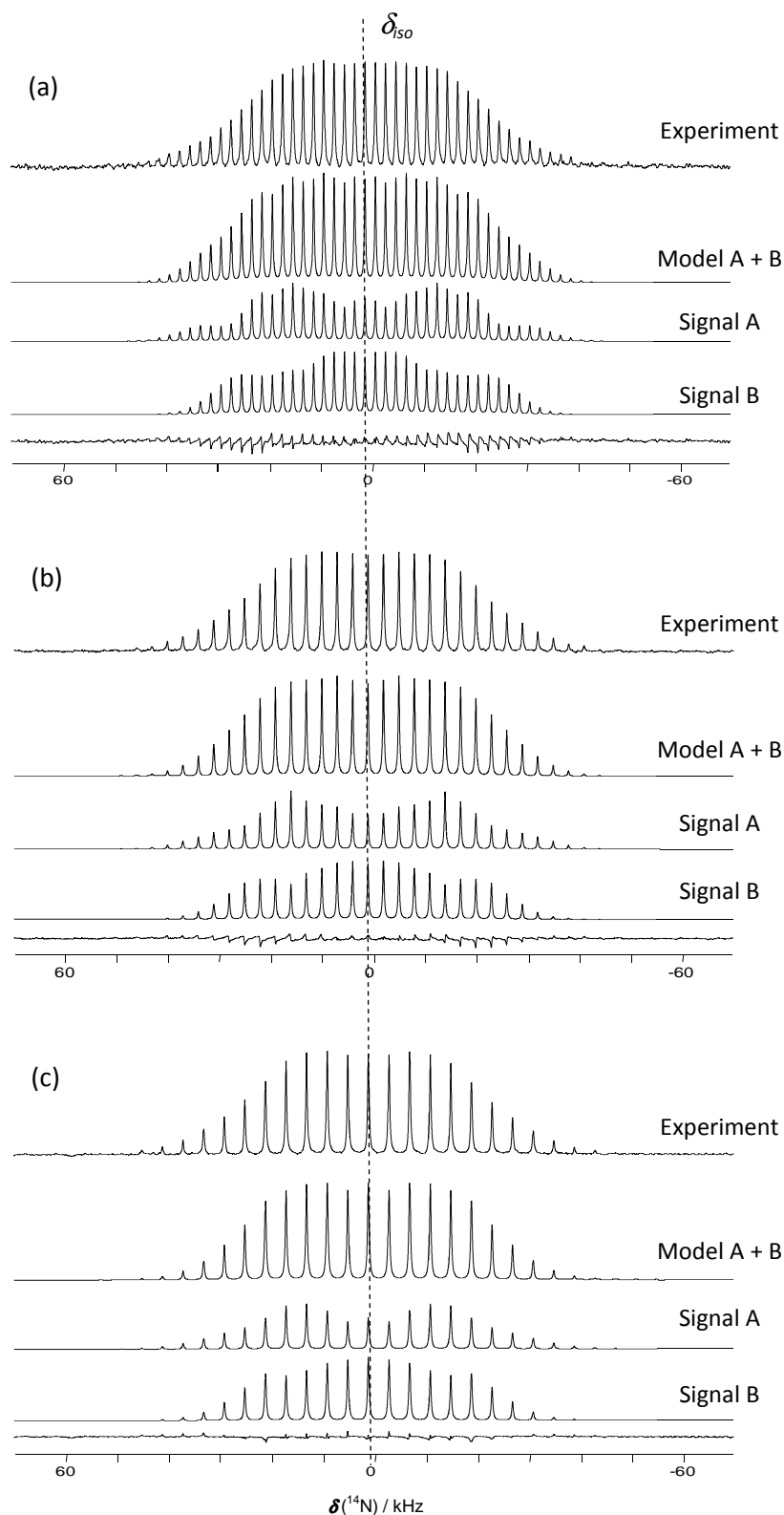
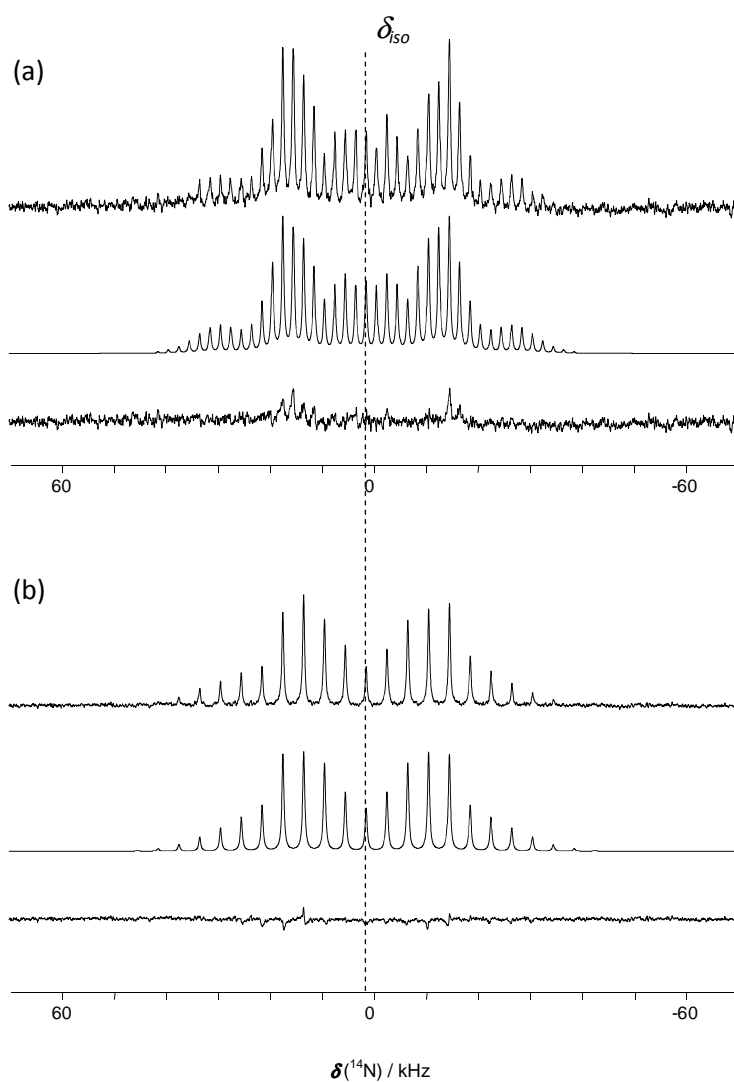


**Fig. S6**  $^{14}\text{N}$  spectra for tetrapropylammonium bromide (TPABr) crystal at different MAS frequencies: (a)  $\nu_{\text{MAS}} = 2$  kHz, (b)  $\nu_{\text{MAS}} = 4$  kHz. The experimental spectra are shown on the top, the modelled spectra on the middle and the differences between them are shown in the bottom.



## 5. $^{14}\text{N}$ NMR parameters estimated from spectrum modelling

### F-MFI

$\nu_{MAS}$ (kHz)	$\delta_{iso}$ (ppm)	$C_Q$ (kHz)	$\eta_Q$
2	25.7	52.8	0.3
3	25.8	52.8	0.3
4	25.5	52.8	0.3

### OH-MFI

$\nu_{MAS}$ (kHz)	$\delta_{iso}$ (ppm)	$\langle C_Q \rangle$ (kHz)
2	26.0	58.1
3	25.7	57.6
4	25.7	58.8

### HT-F-MFI

$\nu_{MAS}$ (kHz)	$\delta_{iso}$ (ppm)	<i>Signal A<sup>a</sup></i>			<i>Signal B<sup>b</sup></i>		
		$C_Q$ (kHz)	$\eta_Q$	Signal area (%)	$C_Q$ (kHz)	$\eta_Q$	Signal area (%)
2	25.5	52.8	0.3	44	45.0	0.7	56
3	25.8	52.8	0.3	42	44.5	0.6	58
4	25.8	52.8	0.3	41	44.7	0.6	59

a. represents the set of quadrupolar parameters of initial F-MFI;

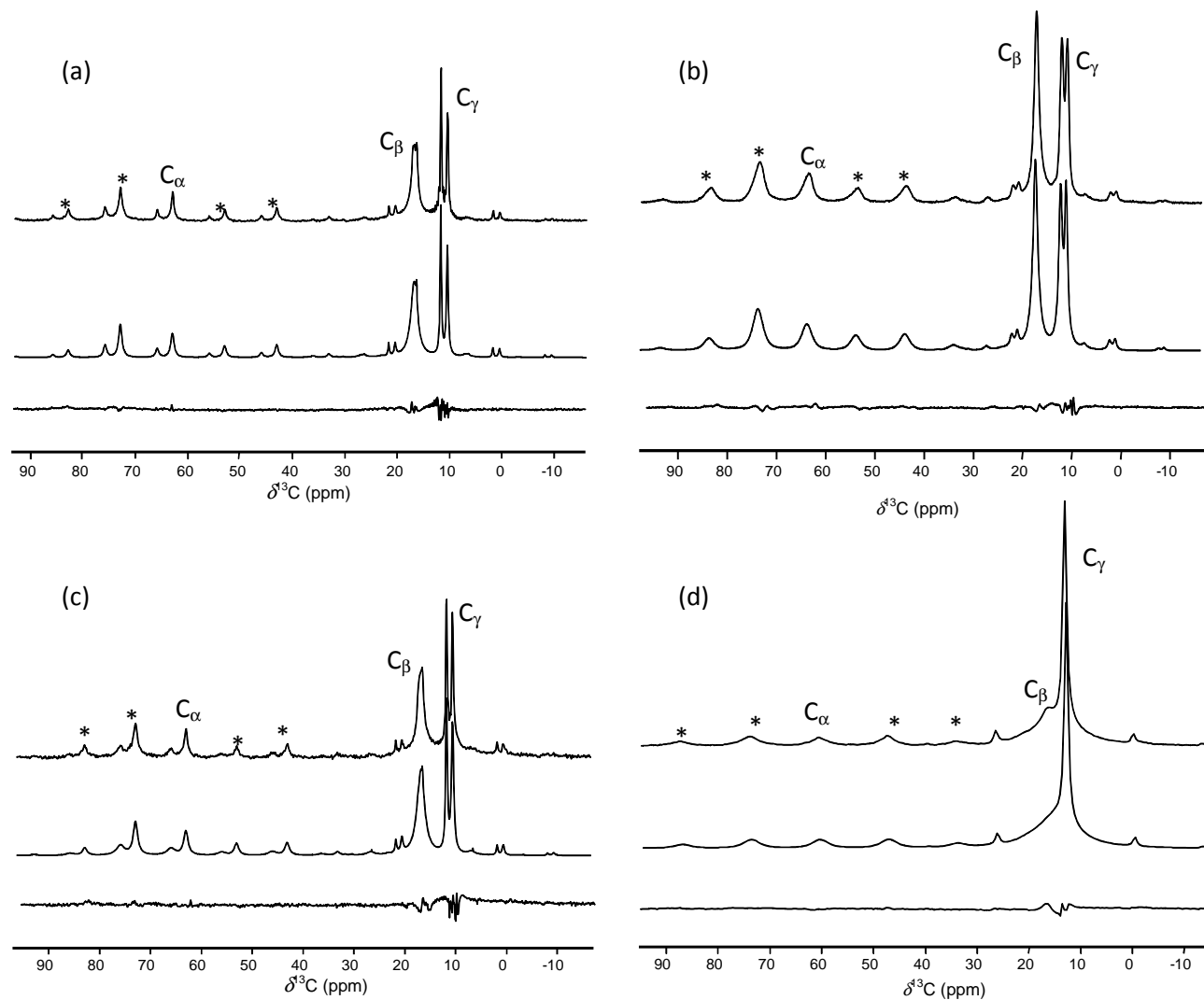
b. represents the new set of quadrupolar parameters after treatment with  $\text{NH}_4\text{OH}$ .

### TPABr

$\nu_{MAS}$ (kHz)	$\delta_{iso}$ (ppm)	$C_Q$ (kHz)	$\eta_Q$
2	30.2	47.8	0.1
4	29.8	48.1	0.1

## 6. $^{13}\text{C}$ NMR spectra

**Fig. S7**  $^{13}\text{C}$  NMR CP-MAS spectra: (a) F-MFI ( $\nu_{\text{MAS}} = 1.5$  kHz), (b) OH-MFI ( $\nu_{\text{MAS}} = 1.5$  kHz), (c) HT-F-MFI ( $\nu_{\text{MAS}} = 1.5$  kHz), (d) TPABr ( $\nu_{\text{MAS}} = 2$  kHz). The experimental spectra are shown on the top, the modelled spectra on the middle and the differences between them are shown in the bottom. (\*) MAS sidebands.



## 7. $^{13}\text{C}$ NMR parameters estimated from spectrum modelling

### F-MFI

Carbon	$\delta_{iso}$ (ppm)	FWHM (ppm)	$\Delta_{CSA}$ (ppm)	$\eta_{CSA}$	Signal area (%)
$\text{C}_\gamma$	10.5	0.41	a	a	16.1
$\text{C}_\gamma$	11.7	0.28	a	a	15.9
$\text{C}_\beta$	16.8	1.52	a	a	37.9
$\text{C}_\alpha$	65.8	0.72	-31.6	0.0	7.6
$\text{C}_\alpha$	62.9	0.76	-31.3	0.2	21.9

a.  $\Delta_{CSA}$  (<10 ppm) can not be determined accurately.

### OH-MFI

Carbon	$\delta_{iso}$ (ppm)	FWHM (ppm)	$\Delta_{CSA}$ (ppm)	$\eta_{CSA}$	Signal area (%)
$\text{C}_\gamma$	10.5	0.71	a	a	15.8
$\text{C}_\gamma$	11.6	0.88	a	a	19.3
$\text{C}_\beta$	16.7	1.18	a	a	30.4
$\text{C}_\alpha$	63.2	2.5	-33.4	0.4	34.4

a.  $\Delta_{CSA}$  (<10 ppm) can not be determined accurately.

### HT-F-MFI

Carbon	$\delta_{iso}$ (ppm)	FWHM (ppm)	$\Delta_{CSA}$ (ppm)	$\eta_{CSA}$	Signal area (%)
$\text{C}_\gamma$	10.6	0.53	a	a	18.2
$\text{C}_\gamma$	11.8	0.36	a	a	14.5
$\text{C}_\beta$	16.8	1.73	a	a	34.8
$\text{C}_\alpha$	66.0	1.91	-31.6	0.0	11.2
$\text{C}_\alpha$	63.0	1.03	-31.3	0.2	21.2

a.  $\Delta_{CSA}$  (<10 ppm) can not be determined accurately.

### TPABr crystal

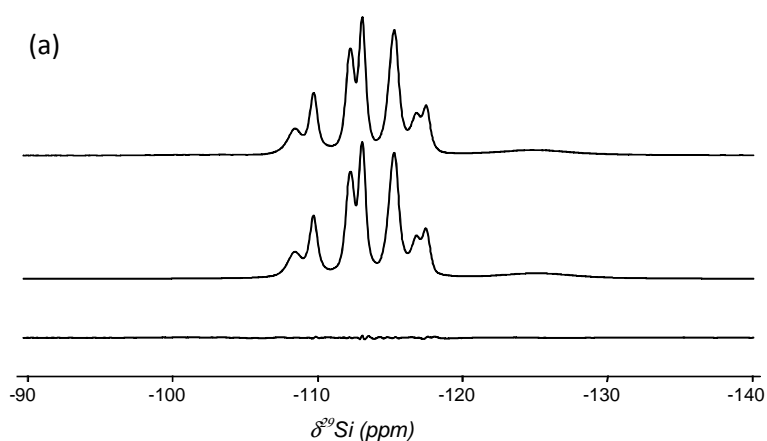
Carbon	$\delta_{iso}$ (ppm)	FWHM (ppm)	$\Delta_{CSA}$ (ppm)	$\eta_{CSA}$	Signal area (%)
$\text{C}_\alpha$	13.1	0.85	a	a	b
$\text{C}_\beta$	15.1	3.64	a	a	b
$\text{C}_\alpha$	60.6	9.32	-37.8	1.0	b

a.  $\Delta_{CSA}$  (<10 ppm) can not be determined accurately.

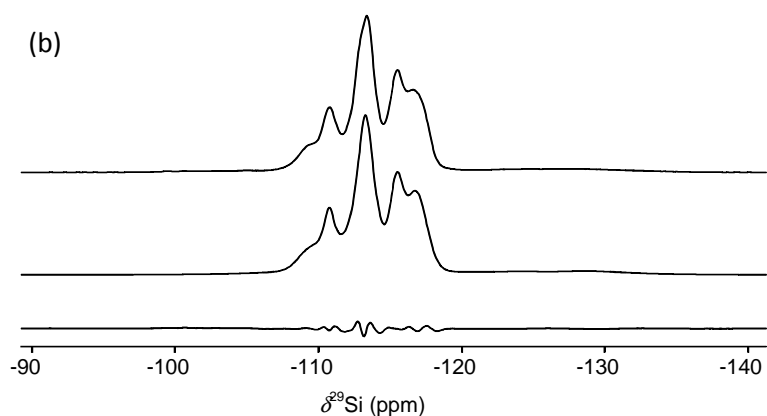
b. The peak area cannot be determined accurately because of the lack of resolution.

## 8. $^{29}\text{Si}$ NMR spectra

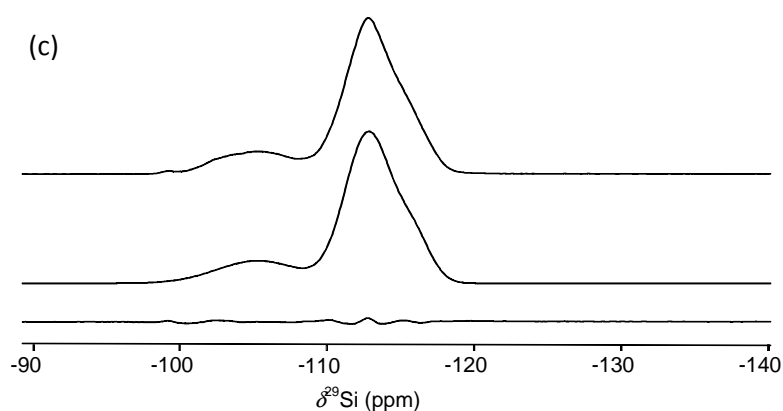
**Fig. S8**  $^{29}\text{Si}$  CP-MAS spectra of: (a) F-MFI, (b) HT-F-MFI, (c) OH-MFI, recorded at  $\nu_{\text{MAS}} = 5$  kHz; the experimental spectra are shown on the top, the modelled spectra on the middle and the differences between them are shown in the bottom. NMR data estimated from spectrum modelling is presented in the left-hand tables.



Peak n°	$\delta_{\text{iso}}$ (ppm)	FWHM (ppm)
1	-108.4	1.13
2	-109.7	0.65
3	-112.1	0.59
4	-112.4	0.45
5	-113.0	0.57
6	-113.2	0.42
7	-114.6	0.49
8	-115.1	0.66
9	-115.4	0.74
10	-116.8	0.82
11	-117.5	0.60
12	-125.2	6.03



Peak n°	$\delta_{\text{iso}}$ (ppm)	FWHM (ppm)
1	-108.1	2.10
2	-109.8	1.17
3	-112.7	1.77
4	-115.2	1.15
5	-116.8	2.03
6	-125.0	7.00
7	-130.1	7.00

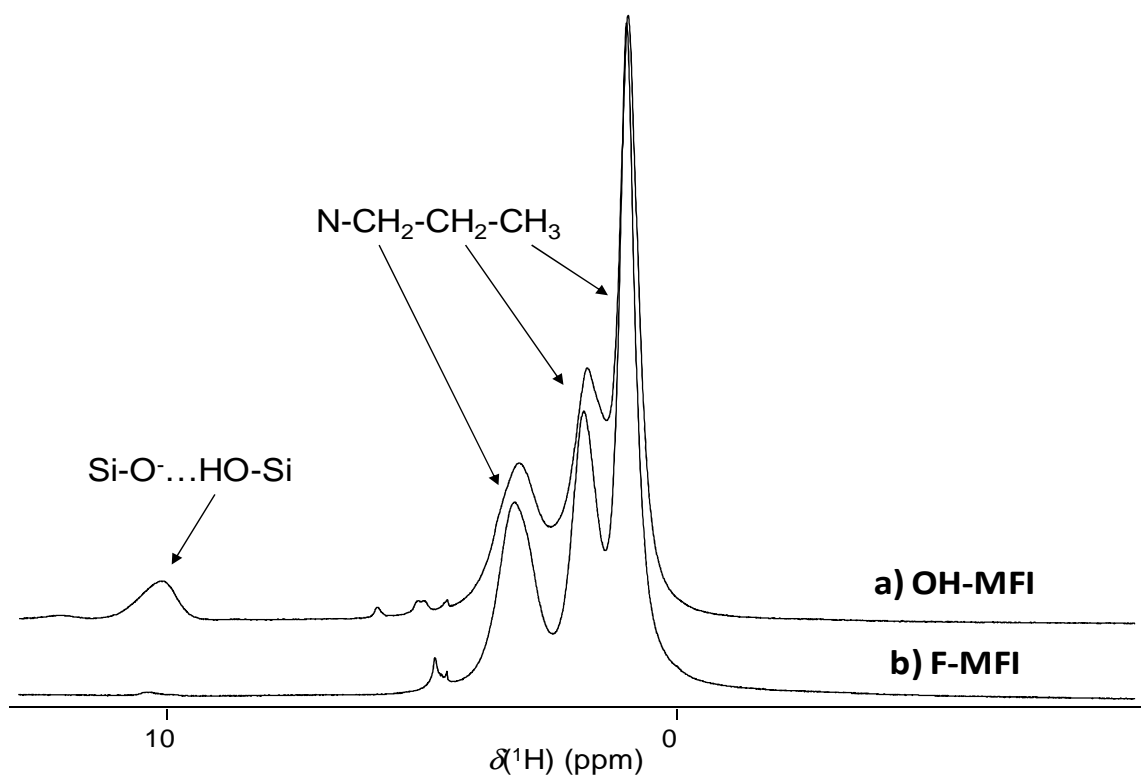


Peak n°	$\delta_{\text{iso}}$ (ppm)	FWHM (ppm)
1	-116.0	3.25
2	-112.3	4.41
3	-103.4	7.87

\*The spectra of F-MFI and HT-F-MFI were modelled using Lorentzian peaks while the spectrum of HO-MFI was modelled using Gaussian peaks.

## 9. Complementary $^1\text{H}$ NMR spectra

**Fig. S9**  $^1\text{H}$  MAS single pulse spectra of: (a) OH-MFI, (b) F-MFI, recorded at fast MAS ( $\nu_{\text{MAS}} = 60$  kHz) and high magnetic field (Larmor frequency of 599.9 MHz). The table presents the related  $^1\text{H}$  chemical shifts and signal area percentages.



Sample / chemical group	$\delta_{\text{iso}}$ (ppm)	Signal area percentage
<b>OH-MFI</b>		
SiO-...HOSi (defects)	10.2	4.6
N-CH <sub>2</sub> (TPA <sup>+</sup> )	3.1	25.6
C-CH <sub>2</sub> -C (TPA <sup>+</sup> )	1.8	25.7
C-CH <sub>3</sub> (TPA <sup>+</sup> )	0.9	44.1
<b>F-MFI</b>		
N-CH <sub>2</sub> (TPA <sup>+</sup> )	3.1	28.9
C-CH <sub>2</sub> -C (TPA <sup>+</sup> )	1.8	24.5
C-CH <sub>3</sub> (TPA <sup>+</sup> )	0.9	46.6

## 10. Complementary $^{19}\text{F}$ NMR spectra

**Fig. S10**  $^{19}\text{F}$  MAS single pulse spectra of F-MFI and HT-F-MFI samples ( $\nu_{\text{MAS}} = 10$  kHz,  $\nu_0 = 564$  MHz). Chemical shift parameters are estimated after spectrum deconvolution.

